Journal of Power Sources 189 (2009) 45–50

Contents lists available at ScienceDirect

Journal of Power Sources

journal homepage: www.elsevier.com/locate/jpowsour

Effects of roasting temperature and modification on properties of Li_2FeSiO_4/C cathode

Li-ming Li, Hua-jun Guo*, Xin-hai Li, Zhi-xing Wang, Wen-jie Peng, Kai-xiong Xiang, Xuan Cao

School of Metallurgical Science and Engineering, Central South University, Changsha 410083, China

ARTICLE INFO

Article history:
Received 29 June 2008
Received in revised form 4 December 2008
Accepted 4 December 2008
Available online 9 December 2008

Keywords:
Lithium ion battery
Cathode
Li_2FeSiO_4

ABSTRACT

Li_2FeSiO_4/C cathodes were synthesized by combination of wet-process method and solid-state reaction at high temperature, and effects of roasting temperature and modification on properties of the Li_2FeSiO_4/C cathode were investigated. The XRD patterns of the Li_2FeSiO_4/C samples indicate that all the samples are of good crystallinity, and a little Fe_3O_4 impurity was observed in them. The primary particle size rises as the roasting temperature increases from 600 to 750 °C. The Li_2FeSiO_4/C sample synthesized at 650 °C has good electrochemical performances with an initial discharge capacity of 144.9 mAh g^{-1} and the discharge capacity remains 136.5 mAh g^{-1} after 10 cycles. The performance of Li_2FeSiO_4/C cathode is further improved by modification of Ni substitution. The $Li_2Fe_{0.9}Ni_{0.1}SiO_4$/C composite cathode has an initial discharge capacity of 160.1 mAh g^{-1}, and the discharge capacity remains 153.9 mAh g^{-1} after 10 cycles. The diffusion coefficient of lithium in Li_2FeSiO_4/C is 1.38×10^{-12} cm^2 s^{-1} while that in $Li_2Fe_{0.9}Ni_{0.1}SiO_4$/C reaches 3.34×10^{-12} cm^2 s^{-1}.

1. Introduction

With the rapid development of large batteries for transportation applications, safety and lifetime issues are becoming large obstacles to the widespread use of many traditional lithium cathode materials [1–3]. While the full implication of the discovery of electrochemical activity in iron-based active materials have completely changed the lithium ion battery landscape in this context [4,5].

The well-known examples are $LiFePO_4$ and Li_2FeSiO_4 distinguished from other materials by their excellent stability [1,6,7]. While Lithium iron orthosilicate have a lowering of the $Fe^{II} \leftrightarrow Fe^{III}$ couple than lithium iron phosphate because of the strong Si–O bonds and the lower electro negativity of Si vs. P. Therefore Li_2FeSiO_4 have a lower electronic band gap and a higher electronic conductivity theoretically than $LiFePO_4$, and it will become a novel cathode material in lithium ion batteries [7,8].

Li_2FeSiO_4 has a theoretical capacity of 166 mAh g^{-1} with a flat discharge voltage at 3.1 V. However, only part of the capacity could be obtained for the original Li_2FeSiO_4, and its capacity decreases considerably at larger current density [1,7,8]. Since Li_2FeSiO_4 was synthesized and characterized by Nytén et al. [1], many efforts had been made to synthesize Li_2FeSiO_4 with better electrochemical performance [9–15].

In Nytén's studies, Li_2FeSiO_4 was prepared by the solid-state reaction of Li_2SiO_3 with $FeC_2O_4{\cdot}2H_2O$. Zaghib et al. [10] synthesized powder samples of Li_2FeSiO_4 by conventional solid-state reaction at moderate temperature. Dominko et al. [11] used a modified Pechini sol–gel process for the synthesis of Li_2FeSiO_4, and he also pointed out that Li_2FeSiO_4 could be prepared using a hydrothermal process [11,12]. In China, a patent about $Li_2Fe_xMn_{2-x}SiO_4$ had been applied by Yang and Li [13].

It is well known that the roasting temperature and modification may greatly affect the crystallinity, stability of phase, homogeneity of particles and electrochemical performances of the cathode. In this paper, we synthesized Li_2FeSiO_4/C by combination of wet-process method and solid-state reaction at high temperature, and investigated the effects of roasting temperature and Ni substitution modification on the structure and properties of Li_2FeSiO_4/C cathodes.

2. Experimental

2.1. Synthesis of $Li_2Fe_{1-x}Ni_xSiO_4$/C

The precursor of $Li_2Fe_{1-x}Ni_xSiO_4$/C ($x = 0$, 0.1, 0.3) was prepared by a solution route. Ball milling process was applied on the precursor in the presence of carbon to coat the particles with carbon, and then $Li_2Fe_{1-x}Ni_xSiO_4$/C composite was synthesized by solid-state reaction. Lithium acetate (99%, AR), $FeC_2O_4{\cdot}2H_2O$ (99%, AR), $Ni(CH_3COO)_2{\cdot}4H_2O$ (99%, AR) and $Si(OC_2H_5)_4$ were used as the

* Corresponding author. Tel.: +86 731 8836633; fax: +86 731 8836633.
E-mail address: ghj.csu@163.com (H.-j. Guo).

0378-7753/$ – see front matter © 2008 Elsevier B.V. All rights reserved.
doi:10.1016/j.jpowsour.2008.12.017

starting materials and were dissolved in ethanol in stoichiometric amounts. The mixture was stirred at 50 °C for 8 h and the ethanol was evaporated. The resulting powders were mixed with sucrose in ethanol and then ground by ball milling. After evaporating the ethanol, the mixture was heated in a horizontal quartz tube at different temperature for 10 h in Ar atmosphere.

2.2. Characterization of $Li_2Fe_{1-x}Ni_xSiO_4/C$

The TG/DTA curve was obtained on a Perkin Elmer TGA 7 thermal analyzer system. The measurement was conducted between 20 and 900 °C at a heating rate of 5 °C/min in N_2 atmosphere.

The samples were characterized by X-ray powder diffraction analysis (XRD) using Cu K radiation ($\lambda = 0.154$ nm). The morphology of the samples was observed by a scanning electron microscope (SEM). The pH of the products was characterized as follows. The Li_2FeSiO_4/C powder was added into distilled water with mass ratio of 1:50, and the mixture was stirred for 10 min. Then the solid was removed by filtration, and pH of the solution was examined with a Mettler Toledo Lp115 pH meter.

2.3. Electrochemical characterization of $Li_2Fe_{1-x}Ni_xSiO_4/C$

The $Li_2Fe_{1-x}Ni_xSiO_4/C$ composite was mixed with acetylene black as electric conductor and poly(vinylidene difluoride) (PVDF) as binder. The $Li_2Fe_{1-x}Ni_xSiO_4/C$ cathode was prepared by spreading the above mixture on an aluminum foil. Charge–discharge tests of the $Li_2Fe_{1-x}Ni_xSiO_4/C$ were performed in coin cells with $Li_2Fe_{1-x}Ni_xSiO_4/C$ cathodes and lithium anodes. A UP 3025 porous membrane of 25 μm thickness was used as a separator, and the electrolyte was 1 mol/L $LiPF_6$ dissolved in a mixture of ethylene carbonate (EC), dimethyl carbonate (DMC) and Methyl–Ethyl Carbonate (EMC) with a volume ratio of 1:1:1. Cells were cycled between 1.5 and 4.8 V at ambient temperature using a LAND battery testing system.

The diffusion coefficient of lithium in $Li_2Fe_{1-x}Ni_xSiO_4/C$ electrodes with different discharge degree was measured by potential step chronoamperometry. The measurement was carried out using a three-electrode cell, which consisted of a $Li_2Fe_{1-x}Ni_xSiO_4/C$ electrode and two lithium electrodes, one as auxiliary electrode and the other as reference electrode. The cell was charged–discharged for two cycles between 1.5 and 4.8 V before the measurement, and then the $Li_2Fe_{1-x}Ni_xSiO_4/C$ electrode was fully charged and discharged to a fixed degree. An anodic overpotential of 200 mV was applied to the $Li_2Fe_{1-x}Ni_xSiO_4/C$ electrode and the response of current was recorded, from which the diffusion coefficient was calculated.

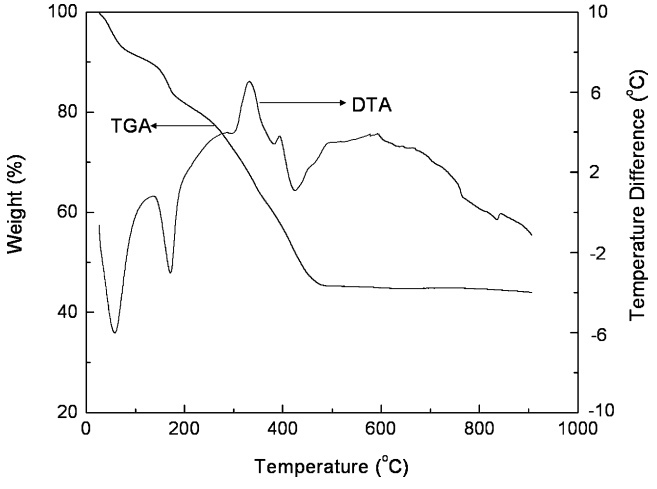

Fig. 1. TGA and DTA curves for the precursor of Li_2FeSiO_4 at a heating rate of 5 °C/min in N_2 atmosphere.

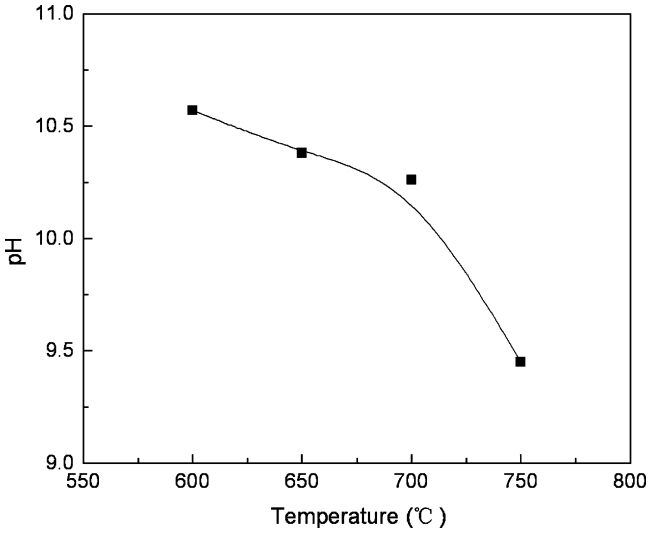

Fig. 2. The pH values of Li_2FeSiO_4/C composites synthesized at different temperatures.

3. Results and discussion

3.1. Effects of roasting temperature on properties of Li_2FeSiO_4/C cathode

In order to investigate the possible reactions occurring in the synthesis of Li_2FeSiO_4, thermo gravimetric analysis and differential thermal analysis were conducted on the precursor in N_2 atmosphere, and the results are shown in Fig. 1. The weight loss curve can be divided into three stages. The first weight loss occurs around 80 °C, and a corresponding endothermic peak is observed in the DTA curve, which is due to the dehydration of physically absorbed water in the sample. The second obvious reduction of weight, corresponding to an endothermic peak, is detected from 160 to 180 °C. It can be attributed to the dehydration of chemically combined water in $Fe(C_2O_4)\cdot 2H_2O$. In the tempera-

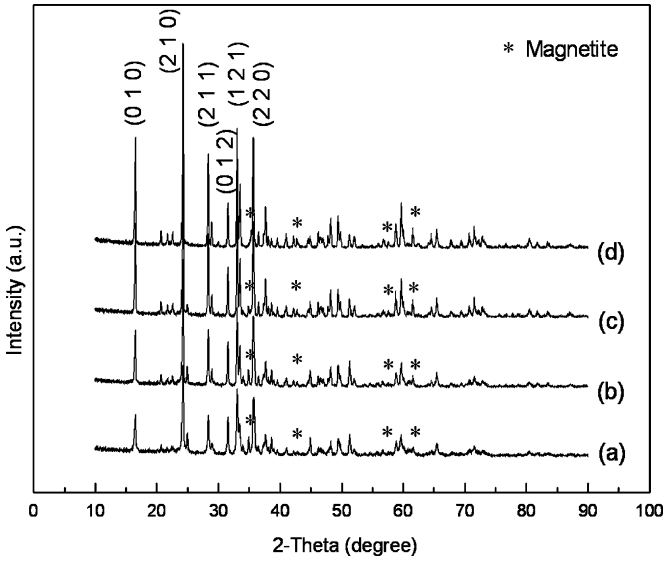

Fig. 3. XRD patterns of Li_2FeSiO_4/C composites synthesized at (a) 600 °C, (b) 650 °C, (c) 700 °C and (d) 750 °C.

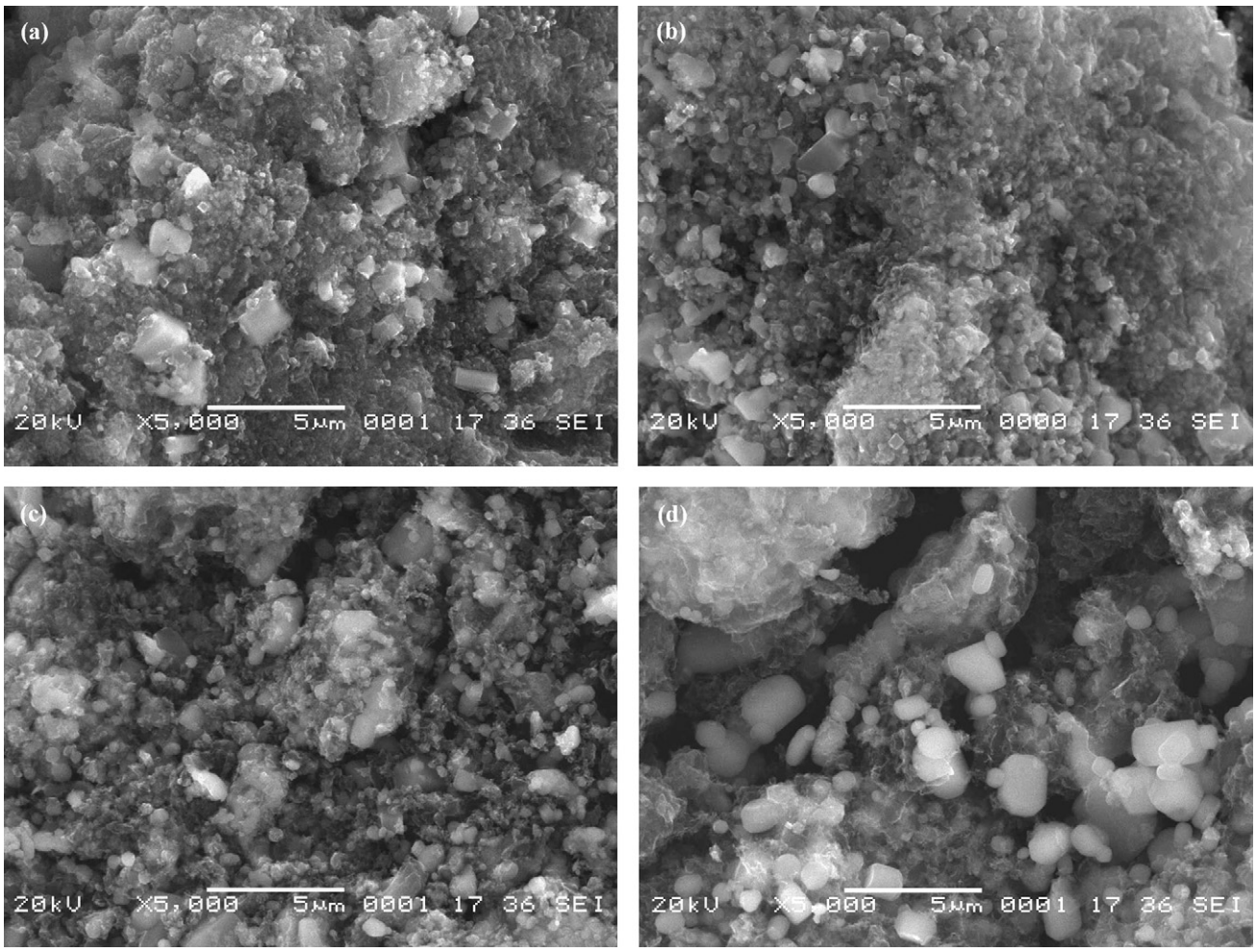

Fig. 4. SEM images of Li_2FeSiO_4/C composites synthesized at (a) 600 °C, (b) 650 °C, (c) 700 °C and (d) 750 °C.

ture range of 290–420 °C, the weight of the sample decreases quickly, which may result from the complicated reactions of LiAc, Fe(C_2O_4) and organosilicon compounds. The weight of the sample keeps nearly constant when the temperature is above 480 °C. According to the results of TG/DTA, the precursor was heat-treated at temperatures between 600 and 750 °C for 10 h in Ar atmosphere.

Fig. 2 shows the pH values of Li_2FeSiO_4/C synthesized at different temperatures. The pH of Li_2FeSiO_4/C materials is related to

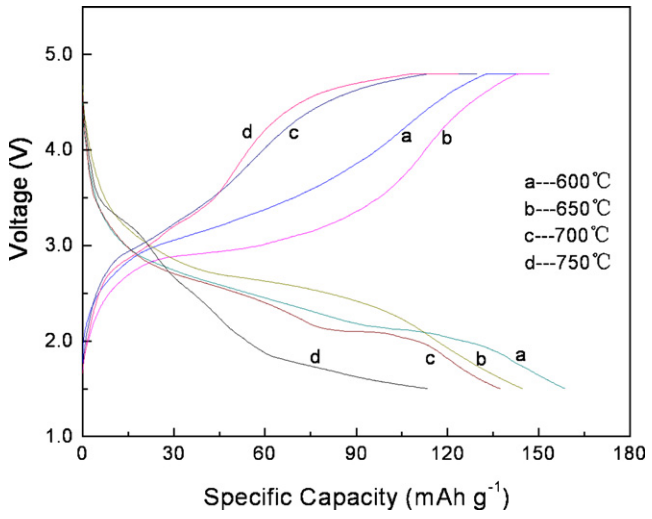

Fig. 5. The charge–discharge voltage profiles of Li_2FeSiO_4/C composites synthesized at different temperatures at C/16 current rate between 1.5 and 4.8 V.

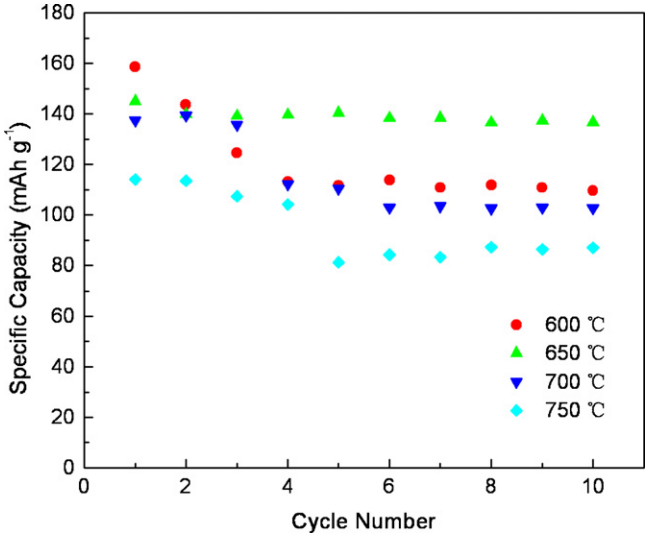

Fig. 6. The cycling performance of Li_2FeSiO_4/C composites synthesized at different temperatures at C/16 current rate between 1.5 and 4.8 V.

the content of residual lithium compounds such as lithium oxide or lithium carbonate which result from the decomposition of the lithium acetate. As shown in the Fig. 2, the pH value of Li_2FeSiO_4/C decreases with increasing the roasting temperature. It is due to the decrease in content of residual lithium oxide or lithium carbonate because the lithium acetate participates in reaction more sufficiently at higher temperature.

Fig. 3 shows the XRD patterns for the Li_2FeSiO_4/C samples synthesized at different temperatures. The narrow diffraction peaks indicate that the samples have good crystallinity. The X-ray diffraction data can be indexed to the orthorhombic unit cell in space group $Pmn2_1$. The lattice constants for the Li_2FeSiO_4/C synthesized at 650 °C have been calculated to be $a = 7.2538$, $b = 6.9767$ and $c = 5.3873$ Å, which is consistent with those reported previously [1,11]. A little Fe_3O_4 impurity has been detected in the samples. As the roasting temperature rises, diffraction peaks of Li_2FeSiO_4 become intense and sharp, suggesting the crystallinity of Li_2FeSiO_4 increases. However, the intensity of diffraction peaks for Fe_3O_4 also rises with increasing the roasting temperature, indicating the content of Fe_3O_4 impurity increases.

Fig. 4 shows SEM images of the Li_2FeSiO_4/C composites synthesized at different temperatures. The powders consist of agglomerates of primary particles. As the roasting temperature increases from 600 to 750 °C, the primary particles size increases, indicating better growth of the primary particles at higher temperature.

Fig. 5 shows charge–discharge voltage profiles of the composites synthesized at different temperatures at C/16 current rate. The discharge capacity increases from 114.0 to 158.7 mAh g^{-1} with decreasing the roasting temperature from 750 to 600 °C. Furthermore, the sample synthesized at 650 °C presents a pair of charge and discharge voltage plateaus at 3.0 and 2.7 V, respectively.

Fig. 6 shows cycling performance of cells at C/16 current rate between 1.5 and 4.8 V. The sample synthesized at 650 °C presents the best cycling stability. It delivers an initial discharge capacity of 144.9 mAh g^{-1}, and the discharge capacity remains 136.5 mAh g^{-1} after 10 cycles, suggesting Li_2FeSiO_4/C composite synthesized at 650 °C has the best electrochemical performances, which can be attributed to its favorable combination of well developed crystal structure, low impurity, and small primary particle size which facilitates the diffusion of lithium ions in the solid. Therefore, a roasting temperature of 650 °C is used in the modification of Li_2FeSiO_4/C cathode.

3.2. Effects of Ni substitution on properties of $Li_2Fe_{1-x}Ni_xSiO_4/C$ cathode

Fig. 7 shows XRD patterns for the $Li_2Fe_{1-x}Ni_xSiO_4/C$ ($x = 0$–0.3) samples synthesized at 650 °C. All the X-ray diffraction data can be indexed to the orthorhombic unit cell in space group $Pmn2_1$. The XRD pattern of $Li_2Fe_{0.9}Ni_{0.1}SiO_4/C$ is very similar to that of Li_2FeSiO_4/C. However, the relative intensity of the diffraction peaks for $Li_2Fe_{0.7}Ni_{0.3}SiO_4/C$ differs greatly from those for other two samples. In the XRD patterns for $Li_2Fe_{0.9}Ni_{0.1}SiO_4/C$ and Li_2FeSiO_4/C, the most intense diffraction peak is observed around 24°, while it occurs around 45° in the XRD pattern for $Li_2Fe_{0.7}Ni_{0.3}SiO_4/C$, suggesting changes in the crystal structure has occurred due to the heavy nickel substitution. The lattice constants of $Li_2Fe_{0.9}Ni_{0.1}SiO_4/C$ have been calculated to be $a = 7.2979$, $b = 6.9733$ and $c = 5.3580$ Å, and those of $Li_2Fe_{0.7}Ni_{0.3}SiO_4/C$ are $a = 8.8719$, $b = 6.7290$ and $c = 5.0254$ Å.

Fig. 8 shows the charge–discharge voltage profile of $Li_2Fe_{1-x}Ni_xSiO_4/C$($x = 0$–0.3) cathodes at C/16 current rate. Among the $Li_2Fe_{1-x}Ni_xSiO_4/C$ cathodes, the $Li_2Fe_{0.9}Ni_{0.1}SiO_4/C$ cathode delivers the largest discharge capacity of 155.5 mAh g^{-1}, and $Li_2Fe_{1-x}Ni_xSiO_4/C$($x = 0$, 0.1) cathodes present remarkable

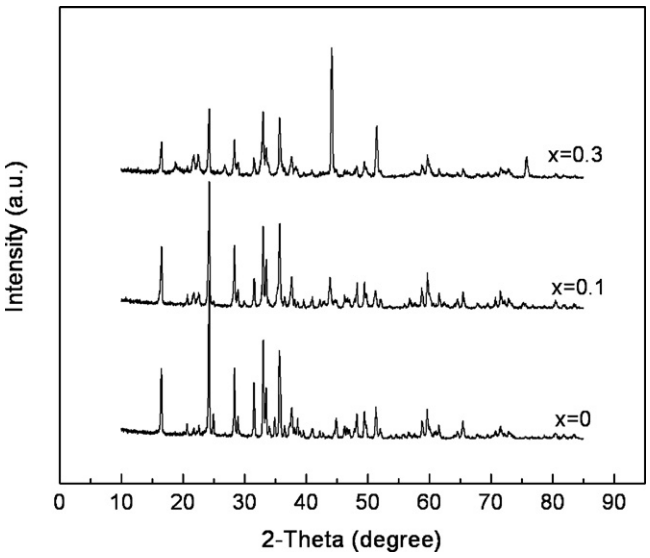

Fig. 7. The XRD patterns for the $Li_2Fe_{1-x}Ni_xSiO_4/C$ ($x = 0$–0.3) samples synthesized at 650 °C.

charge and discharge voltage plateaus. So Li_2FeSiO_4/C and $Li_2Fe_{0.9}Ni_{0.1}SiO_4/C$ are used in the following research. Fig. 9 shows the cycling performance of $Li_2Fe_{1-x}Ni_xSiO_4/C$($x = 0$, 0.1) cathodes at C/16 rate between 1.5 and 4.8 V. Compared with Li_2FeSiO_4/C, $Li_2Fe_{0.9}Ni_{0.1}SiO_4/C$ shows better cycling stability. It has an initial discharge capacity of 160.1 mAh g^{-1}, and the discharge capacity remains 153.9 mAh g^{-1} after 10 cycles. Therefore, the $Li_2Fe_{0.9}Ni_{0.1}SiO_4/C$ cathode has the best charge–discharge performance among the $Li_2Fe_{1-x}Ni_xSiO_4/C$($x = 0$, 0.1, 0.3) cathodes, which may be due to its improved conductivity compared to the Li_2FeSiO_4/C and the better crystal structure compared to the $Li_2Fe_{0.7}Ni_{0.3}SiO_4/C$, respectively.

3.3. Kinetics of Li ion insertion in $Li_2Fe_{1-x}Ni_xSiO_4/C$ cathode

AC impedance measurement was carried out using three-electrode cells with Li_2FeSiO_4/C cathodes of different state of charge (SOC), and the results are shown in Fig. 10. The impedance plot consists of a depressed semicircle and an inclined line. The intercept at

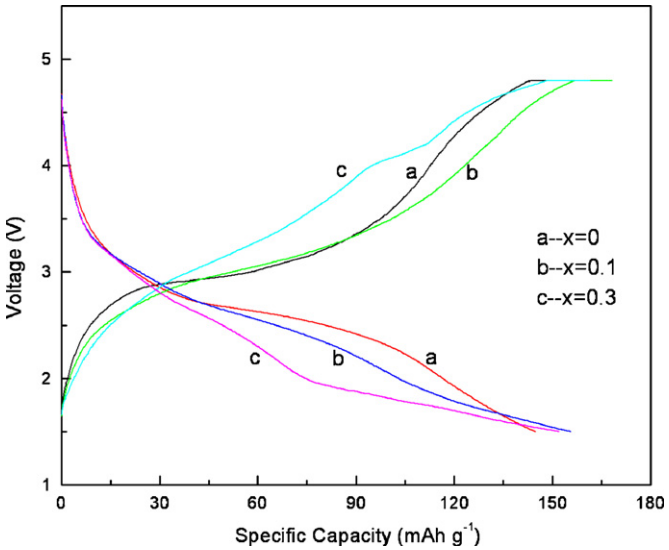

Fig. 8. The charge–discharge voltage profile of $Li_2Fe_{1-x}Ni_xSiO_4/C$ ($x = 0$–0.3) cathodes at C/16 current rate between 1.5 and 4.8 V.

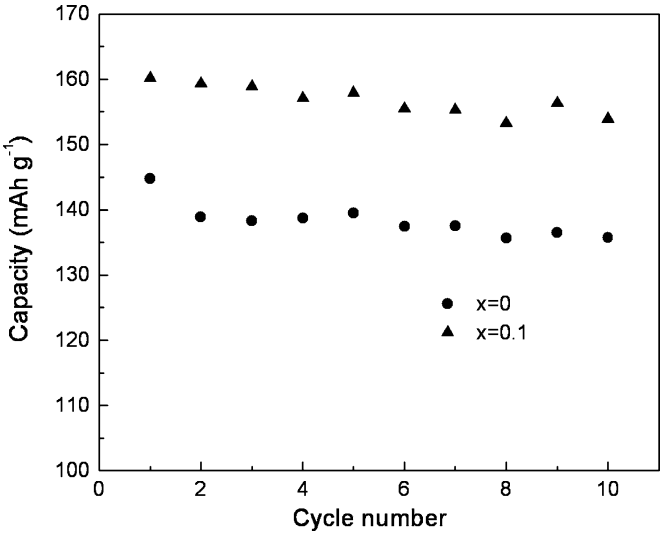

Fig. 9. The cycling performance of $Li_2Fe_{1-x}Ni_xSiO_4/C$ ($x = 0$, 0.1) cathodes at C/16 current rate between 1.5 and 4.8 V.

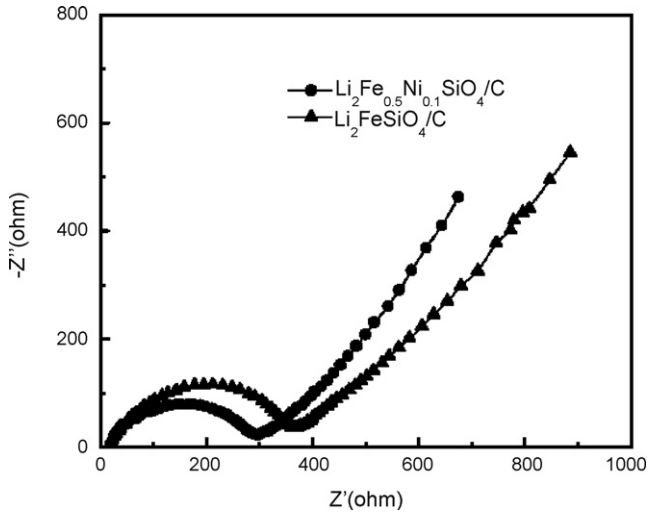

Fig. 11. AC impedance of $Li_2Fe_{1-x}Ni_xSiO_4/C$ ($x = 0$, 0.1) electrodes with 50% SOC.

the Z' axis in high frequency corresponds to the ohmic resistance (R_e), which represents the resistance of the electrolyte. The semicircle in the middle frequency range indicates the charge transfer resistance (R_{ct}). The inclined line in the low frequency represents the Warburg impedance (Z_w), which is associated with lithium ion diffusion in the cathode particles [16]. In this work, the R_e values are almost the same throughout the experiments due to the same electrolyte and fabrication parameters, and they are much smaller and almost negligible compared with R_{ct} since the cells are assembled with rich electrolyte. As shown in Fig. 10, the R_{ct} of the (Li_2FeSiO_4/C)/electrolyte interface at full charge degree (100% SOC) can be evaluated to be about 640 Ω. While those for the cells at 50% and 0% SOC are about 810 and 1000 Ω, respectively, suggesting the R_{ct} increases obviously with cell discharging.

Fig. 11 shows the impedance spectra for cells with $Li_2Fe_{1-x}Ni_xSiO_4/C$($x = 0$, 0.1) cathodes of 50% SOC. The slopes of the straight lines in low frequency region are similar for both cathodes. However, obvious difference in R_{ct} of the cathodes can be observed. The R_{ct} at the (Li_2FeSiO_4/C)/electrolyte interface was about 350 Ω, while that at the ($Li_2Fe_{0.9}Ni_{0.1}SiO_4/C$)/electrolyte interface decreases to about 300 Ω.

The response of current (i) with time (t) under constant potential step for Li_2FeSiO_4/C and $Li_2Fe_{0.9}Ni_{0.1}SiO4/C$ is shown in Fig. 12a.

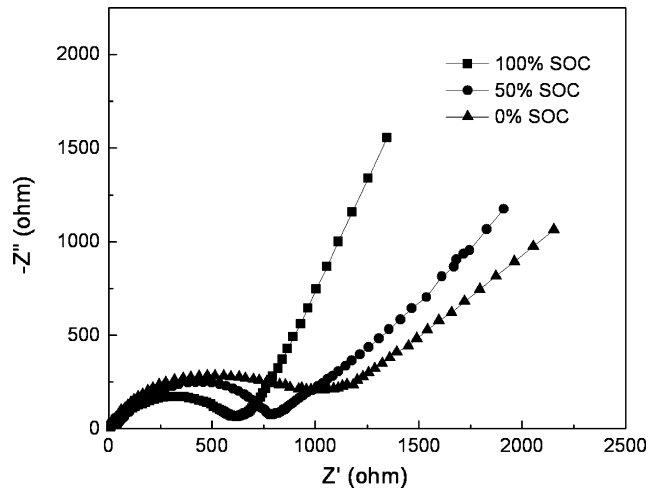

Fig. 10. AC impedance of Li_2FeSiO_4/C electrodes with different state of charge.

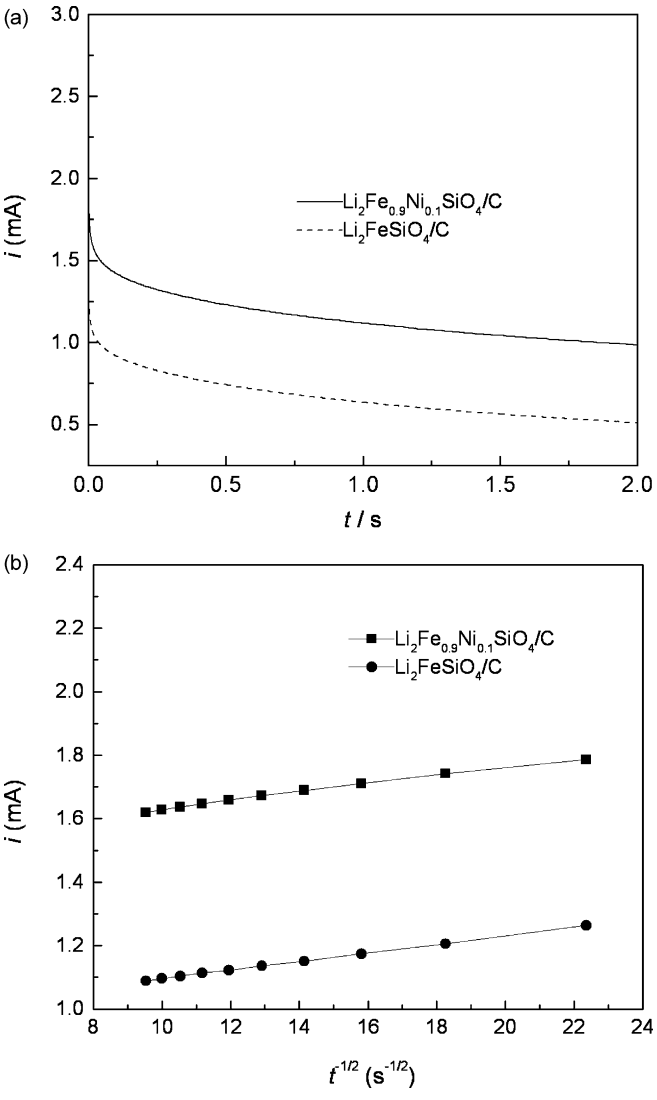

Fig. 12. Response of current for $Li_2Fe_{1-x}Ni_xSiO_4/C$ ($x = 0$, 0.1) under potential step. (a) i vs. t profiles; (b) i vs. $t^{-1/2}$ profiles.

Table 1
Results for diffusion coefficient of lithium in $Li_2Fe_{1-x}Ni_xSiO_4/C$ cathodes.

Sample	k (A s$^{1/2}$)	b (A)	D_{Li} (cm^2 s^{-1})
Li_2FeSiO_4/C	1.377×10^{-2}	9.563×10^{-4}	1.38×10^{-12}
$Li_2Fe_{0.9}Ni_{0.1}SiO_4/C$	1.382×10^{-2}	1.4935×10^{-3}	3.34×10^{-12}

Based on them, i vs. $t^{-1/2}$ profiles were derived as shown in Fig. 12b. With increase of $t^{-1/2}$, the response current rose linearly, and the slope k and intercept b for the lines were obtained. The $Li_2Fe_{1-x}Ni_xSiO_4/C$(x = 0, 0.1) particles have an average diameter of approximate 0.3 μm according to the SEM images. The diffusion coefficients calculated according to equation $D = b^2R_0^2/\pi k^2$ [17] are listed in Table 1. The diffusion coefficient of lithium in Li_2FeSiO_4/C is 1.38×10^{-12} cm^2 s^{-1}, while that in $Li_2Fe_{0.9}Ni_{0.1}SiO_4/C$ reaches 3.34×10^{-12} cm^2 s^{-1}.

In conclusion, compared with Li_2FeSiO_4/C composite, $Li_2Fe_{0.9}Ni_{0.1}SiO_4/C$ composite shows higher discharge capacity, better cycling stability and lager diffusion coefficient of lithium ion in the solid. It may be attributed to the improvement on structure of the composite by modification of Ni substitution.

4. Conclusions

By combination of wet process method and solid-state reaction at high temperature, Li_2FeSiO_4/C cathode samples were synthesized. According to results of TG/DTA analysis, heat treatment of the precursor was conducted in the range of 600–750 °C.

As the roasting temperature increases from 600 to 750 °C, the primary particle size rises and the discharge capacity of Li_2FeSiO_4/C cathode decreases from 158.7 to 114.0 mAh g^{-1}. The Li_2FeSiO_4/C sample roasted at 650 °C has the best electrochemical performances with an initial discharge capacity of 144.9 mAh g^{-1} and a capacity retention ratio of 94.2% at the 10th cycle.

Compared with the undoped Li_2FeSiO_4/C cathode, the $Li_2Fe_{0.9}Ni_{0.1}SiO_4/C$ composite cathode has a better electrochemical performance with an initial discharge capacity of 160.1 mAh g^{-1}, and the discharge capacity remains 153.9 mAh g^{-1} after 10 cycles. The diffusion coefficient of lithium increases from 1.38×10^{-12} cm^2 s^{-1} to 3.34×10^{-12} cm^2 s^{-1} with Ni substitution.

Acknowledgements

The financial support by the National Basic Research Program of China (2007CB613607) are acknowledged.

References

[1] A. Nytén, A. Abouimrane, M.L. Armand, Electrochem. Commun. 7 (2005) 156.
[2] R. Oesten, U. Heider, M. Schmidt, Solid State Ionics 148 (2002) 391.
[3] J. Arai, H. Katayama, H. Akahoshi, J. Electrochem. Soc. 149 (2002) A217.
[4] P. Deniard, A.M. Dulac, X. Rocquefelte, V. Grigorova, O. Lebacq, A. Pasturel, S. Jobic, J. Phys. Chem. Solids 65 (2004) 229.
[5] F. Zhou, M. Cocossioni, K. Kang, G. Ceder, Electrochem. Commun. 6 (2004) 1144.
[6] W. Ojczyk, J. Marzec, J. Power Sources 173 (2007) 700.
[7] P. Larsson, R. Ahuja, A. Nytén, J.O. Thomas, Electrochem. Commun. 8 (2006) 797.
[8] R. Dominko, M. Bele, M. Gaberscek, M. Remskar, D. Hanzel, J.M. Goupil, S. Pejovnik, J. Jamnik, J. Power Sources 153 (2006) 274.
[9] M.E. Arroyo, J.M. Amores, J.G. Martínez, E. Morán, J.M. Tarascon, M. Armand, Solid State Ionics 170 (2008) 1758.
[10] K. Zaghib, A.A. Salah, N. Ravet, A. Mauger, F. Gendron, C.M. Julien, J. Power Sources 160 (2006) 1381.
[11] R. Dominko, M. Bele, M. Gaberscek, A. Meden, M. Remskar, J. Jamnik, Electrochem. Commun. 8 (2006) 217.
[12] R. Dominko, D.E. Conte, D. Hanzel, M. Gaberscek, J. Jamnik, J. Power Sources 178 (2008) 842.
[13] Y. Yang, Y.X. Li, CN 1803608A, (2006) 7.
[14] R. Dominko, M. Bele, J.M. Goupil, M. Gaberscek, D. Hanzel, I. Arcon, J. Jamnik, Chem. Mater. 19 (2007 2960).
[15] R. Dominko, J. Power Sources 184 (2008) 462.
[16] F. Gao, Z.Y. Tang, Electrochim. Acta 53 (2008) 5071.
[17] H.J. Guo, X.H. Li, X.M. Zhang, H.Q. Wang, Z.X. Wang, W.J. Peng, New Carbon Mater. l22 (2007) 8.